Egypt. J. Chem. **Vol. 65,** No. SI13B pp. 1477 - 1487 (2022)

Egyptian Journal of Chemistry

http://ejchem.journals.ekb.eg/

Anticancer effect of Sorafenib-loaded iron oxide nanoparticles and bee venom on some genes expression in hepatocellular carcinoma

Rana A. A. Nagy [a], Heba K.A. Elhakim[a] ,Mona H. Mohamed [c], Mie afify [d], Mohamed D.E. Abd El-Maksoud [d], Abdel Razik H. Farrag [e], Doaa S. R. Khafaga [a,f], Eid,M.M [b*]

[a] *Biochemistry Division, Faculty of Science, Cairo University, Giza, 12613, Egypt*

[b] *Spectroscopy Department, National Research Centre, Dokki, Giza, 12622, Egypt*

[c] *Department of Chemistry, Faculty of Science, Cairo University, Giza, 12613, Egypt*

[d] *Department of Biochemistry, Genetic Engineering and Biotechnology Research Division, National Research Centre, Dokki, Giza, 12622, Egypt*

[e] *Professor of Histology and Histochemistry, Pathology Department, Medical Research Division, National Research Centre, Dokki, Giza, 12622, Egypt*

[f] *Faculty of Medicine, Galala University, Suez, 43511, Egypt*

Abstract

Objective Superparamagnetic iron oxide@silver@chitosan core-shell nanoparticles could be a promising anticancer agent. This experiment was designed to compare bee venom, a natural substance that has been utilized as a traditional medicine for the treatment of cancer, to a new strategy in the recession of hepatocellular carcinoma utilizing Fe2O3@Ag@Cs nanoparticles. **Methods**: Group I is the negative control group, and Group II is the positive control group. The positive control group received a single intraperitoneal injection of 60 mg/kg b.wt. diethyl nitrosamine, followed by two days of carbon tetrachloride diluted with paraffin oil. Group III was given sorafenib twice a week by gavage for one month, Group IV was given Fe2O3@Ag@Cs core shell NPs, Group V was given Fe2O3@Ag@Cs core shell NPs loaded with sorafenib, and Group VI was given bee venom. **Results:** In comparison between the treated groups and the positive control group, biochemical data demonstrated a highly significant drop in ALT, AST, ALP, and AFP after treatment, as well as significant down-regulation in the DTL gene, while DUSP1, SOCS2, and NFKB1A exhibited up-regulation after treatment. **Conclusion:** Because there was a significant variation in the fold of expression in studied genes, which related to the degree of pathogenicity of hepatocellular carcinoma and gave good valuable insights about the progression of HCC and prognosis, loading sorafenib on Fe2O3@Ag@Cs core-shell NPs is superior to bee venom in the treatment of hepatocellular carcinoma.

Keywords Hepatocellular carcinoma, Bee venom, Sorafenib, Drug delivery, γ Fe_2O_3@Ag@Cs core shell NPs.

1. Introduction

Hepatocellular carcinoma (HCC) is the fifth most common cancer in the world and the third major cause of cancer-related deaths **(Bishayee and Dhir 2009)**. The majority of HCC cases are associated with liver cirrhosis (Aebi 1984). Nanoparticle-based cancer treatments offer a novel method of delivering anticancer drugs directly to tumor cells and to drug-resistant cancer cells at effective quantities, resulting in enhanced target cell accumulation and fewer side effects from high-dose chemotherapy **(Kumar et al. 2010; Denora et al. 2012; Laquintana et al. 2014; Fanizza et al. 2016; Valente et al. 2016)**. Noble metal nanoparticles are a new form of functional material that is gaining popularity in biological applications such as antimicrobials, cancer therapy, and bioimaging **(Zheng et al. 2016, 2017)**. **(Zhang et al. 2014; Song et al. 2016; Goswami et al. 2017)**. Magnetic NP-based delivery systems, in example, offer an intriguing way for localizing pharmaceuticals in the body employing magnetic forces that operate over a long range and are unaffected by most biological tissues **(Alexiou et al. 2000; Owen et al. 2015)**. Silver is commonly employed in biological applications due to its properties. Silver nanoparticles have an advantage in amassing pharmacological targets in macrophages, and they can swiftly infiltrate mammalian cells and cause toxicity due to their high affinity for biological molecules **(Evanoff and Chumanov 2005)**. In the

*Corresponding author e-mail: rana_assem@yahoo.com

Receive Date: 16 May 2022, Revise Date: 11 March 2023, Accept Date: 18 July 2022

DOI: 10.21608/EJCHEM.2022.138553.6104

diagnosis and treatment of cancer, nanomaterials are used. Silver nanoparticles are also employed in cancer treatment. Physical, chemical, and biological approaches are all used to make silver nanoparticles. Biological approaches are referred regarded as "green science" since they are environmentally benign, less harmful, clean, and time efficient. Core shell nanoparticles have been studied extensively, particularly as multimodal nanoparticles for medical use **(Ravichandran et al. 2016; Redolfi Riva et al. 2017; Stafford et al. 2018; Srinivasan et al. 2018)**. According to clinical trials, sorafenib, an oral multikinase inhibitor, exhibits antiproliferative, antiangiogenic, and/or proapoptotic actions that reduce tumor growth and damage tumor microvasculature. It has the potential to greatly improve the survival rates of liver cancer patients. Sorafenib, on the other hand, has a number of disadvantages, including a low water solubility and a short in vivo half-life. Furthermore, liver cancer may develop resistance to sorafenib and become resistant to anti-angiogenic therapy, leading to a high recurrence rate **(Carmeliet and Jain 2011; Semenza 2012; Jain 2013)**. Using enhanced permeability and retention effects such as biodegradable polymeric nano carriers, a new technology was developed recently to improve the solubility of hydrophobic drugs, lengthen the half-life, and improve the targeted enrichment performance of pharmaceuticals to tumors. **(Ferrari 2005; Chauhan and Jain 2013; Cheng et al. 2017; Shi et al. 2017; Liu et al. 2017, 2019; Kydd et al. 2017; Luo et al. 2019); Ferrari 2005; Chauhan and Jain 2013; Cheng et al. 2017; Shi et al. 2017; Liu et al. 2017; Liu et al. 2017; Liu et al. 2017**). Bee venom is a complex mixture of active peptides, enzymes, and amines, according to experts. Histamine, catecholamines, polyamines, melittin, and phospholipase A2 are the main components of bee venom **(Habermann 1972)**. Induction of apoptosis, necrosis, cytotoxicity, and reduction of proliferation in a range of cancer cell types, including prostate, breast, lung, liver, and bladder, have all been related to BV in studies **(Heinen and da Veiga 2011)**. The goal of this work is to assess the anticarcinogenic potency of Fe2O3@Ag@Cs core shell NPs and to increase the therapeutic impact of sorafenib by loading it on a Fe2O3@Ag@Cs core shell, while comparing it to the anticancer effect of bee venom natural product.

2. Materials and methods

2.1. Biologically synthesis of drug delivery system

The deposition of Ag atoms onto the seeds of the Fe2O3 via regulated reduction of Ag precursor in a growth solution containing iron oxide nanoparticles is the synthesis method for nanoparticles (Eid, M. M. et al. 2018). Equal amounts of Fe2O3@Ag@Cscore shell nanoparticles and sorafenib were combined and pulverized in a mortar, then dissolved in 25 ml of sterile distal water, followed by sonication at various times to determine the ideal time for drug allocation on the nanoparticles, and dried overnight at 40°C.

2.2. Characterization of nanoparticles

Fourier transform infrared spectroscopy research was performed on the manufactured nano-core shell to analyze the molecular structure of the nanocomposite and the capping layer that decorates the nanoparticles to better understand the manufacturing procedure. The transmission spectrum for the MID-Far range was collected using diamond cells. A Vertex 70 Bruker Transform Infrared spectrophotometer with a 1 cm-1 resolution in the range of 4000 to 400 cm-1 was used to capture the spectra. HRTEM (JEM-2100HR, Japan) at 200 KeV was used to analyze the shape and structure of the samples. XRD investigations were performed on a Bruker D-8 powder X-ray diffractometer with Cu K radiation (=0.15418 nm) throughout a 2°-90° range with a 0.02° step on a Bruker D-8 powder X-ray diffractometer. The dynamic light scattering (DLS) method was used to calculate the zeta potential using a PSS-NICOMP 380-ZLS, USA.

2.3. Animal model

42 male albino rats (18010 g) were supplied by the National Research Centre (NRC) Dokki in Giza, Egypt. Seven rats per cage were maintained in polypropylene cages with stainless steel wire coverings. Rats were housed in a typical laboratory setting with a 12-hour light/dark cycle, a standard diet, and water. The current protocol (CU/I/S/101/17) was authorized after all animal operations were completed in compliance with the experimental animal care recommendation criteria. Negative control group (group I), Group (II): HCC was used to induce the positive control group. HCC rats were given sorafenib (10 mg/kg b.wt.) for 15 days in Group III (El-Ashmawy et al. 2017). HCC rats were given Fe2O3@Ag@Cs core shell NPs (10 mg/Kg b.wt.) for 15 days in Group IV. HCC rats were given sorafenib loaded on Fe2O3@Ag@Cs core shell NPs (10 mg/Kg b.wt.) for 15 days, and HCC rats were given bee venom (10 mg/Kg b.wt.) for 15 days in Groups V and VI. After scarifying the animals, the liver index was determined as follows: liver weight (g)/ final body weight (g) X 100.

2.4. Histopathological examination

The specimens were washed in tap water, dehydrated in ethanol, clarified in xylene, and embedded in paraffin wax (melting point 56-60oC). Haematoxylin and eosin were used to stain 6 mm thick sections (Liu

et al. 2017). This procedure required staining the paraffin slices with Harris haematoxylin for 5 minutes. Blued in running water, then stained for 2 minutes with 1 percent watery eosin, rinsed in water, dehydrated, cleaned, and mounted with canada balsam. The nuclei were blue, while the cytoplasm ranged from pink to red in color.

2.5. Biochemical assay

Liver function tests were done as (ALT and AST) **(Henry et al. 1960)**, bilirubin (Bil), alkaline phosphatase (ALP), and alpha feto protein (AFP) **(Young 1997)**, using spectrum kits, in addition to liver tissue antioxidant as malonaldehyde (MDA) **(Ohkawa et al. 1979)**, nitric oxide (NO) **(Sayed 2019)**, catalase assay (CAT) **(Aebi 1984)**, and superoxide dismutase (SOD) **(Nishikimi et al. 1972)**, glutathione peroxidase (Paglia and Valentine 1967; Nishikimi et al. 1972; Habig et al. 1974; Meng et al. 2018), glutathione S-transferase (GST) **(Paglia and Valentine 1967)** using bio diagnostic kits.

2.6. Biomarker genes for HCC diagnosis and treatment

TRIzol® extraction chemical was used to isolate total genomic RNA from all treated animals' liver tissues (Invitrogen). Once the isolation procedures were completed, the RNA pellet was stored in DEPC-treated water. An RNAase-free DNAase kit was used to digest any potential DNA residues in the extracted RNA pellet (Invitrogen, Germany). RNA aliquots were either stored at -20°C or used for reverse transcription immediately **(Shawi et al. 2015).** The First Strand cDNA Synthesis Kit (Revert AidTM, MBI Fermentas) was used to generate the cDNA copy from liver tissues via reverse transcription (RT). The cDNA copy of the liver genome was obtained using an RT reaction schedule that included 10 minutes at 25°C, one hour at 42°C, and five minutes at 95°C. Finally, cDNA copies were placed in tubes on ice and used for cDNA amplification (Ding et al. 2017). The qRT-PCR experiments were performed with the SYBR® Premix Ex TaqTM kit (TaKaRa, Biotech. Co. Ltd.) and generated cDNA copies from liver tissues. For each reaction, a melting curve profile was created. Table 1 shows how the expression of the housekeeping gene was used to standardize the quantitative values of the target genes. In comparison to the β-actin gene, the quantitative values of the individual genes were determined using the 2CT method.

1.1. Analytical statistics

Data of continuous variables expressed as mean standard deviation (Mean ± SD) of 8 animals were entered and analyzed using a standard computer programmed (SPSS for Windows, release 25.0, IBM SPSS Inc., USA). One-way ANOVA, Turkey's honestly significant difference (HSD) test, and statistically significant differences were considered as P 0.05.

3. Results and discussion

Hepatocellular carcinoma (HCC) is the most common type of primary liver cancer, accounting for up to 90% of all primary hepatic malignancies (Kj et al. 2015). HCC develops from hepatocytes in the liver parenchyma and is followed by liver cirrhosis and the formation of irregular structural nodules with surrounding fibrosis 80 percent of the time **(Moradpour and Blum 2005)**. At the moment, a number of iron oxide nanoparticles (NPs) have been approved in clinical trials **(Arruebo et al. 2007; Prijic and Sersa 2011; Pablico-Lansigan et al. 2013).** Sorafenib, a pan tyrosine kinase receptor inhibitor, is the first and only chemotherapeutic drug clinically approved for patients with advanced HCC **(Fattovich et al. 2004; Kj et al. 2015).** Sorafenib's low water solubility limits its use to specific applications. Patients with HCC may benefit from the development of a tumor-targeted drug delivery system that concentrates sorafenib at the cancer site, improving bioavailability, efficacy, and safety. The green approach for nanoparticle synthesis, as well as the drug structure and drug loading on the NP, are confirmed by Fourier transform infrared spectroscopy. Figure 1 depicts the FTIR transmission spectrum of the vibrational bands in the nanocomposite and, as a result, the development of the Fe2O3@Ag@Cs functionalized with chitosan. Previous research has linked the absorption bands at 550 and 450 cm-1 to the vibrations of the Fe–O bond and has thus been used to validate the creation of iron oxide nanoparticles **(Marková et al. 2012; Mascolo et al. 2013; Zielonka and Klimek-Ochab 2017)**. This band confirms the formation of Fe2O3 as previously demonstrated by **Zhang et al. 2013**. According to **Du et al. (2010)**, the complexity of maghemite's unit cell versus maghemite causes the formation of more Raman and infrared active phonons **(du et al. 2010; Zhang et al. 2013)**. The appearance of the three characteristic peaks of SFB CF2 at 849, 700, and 550 cm-1 and the CN peak at 1725 cm-1 with a significant decrease of the peak at 849 cm-1 confirms the drug's allocation on the nanocomposite. The formation of spherical nanoparticles with particle sizes in the range of 20-30 nm and 80 nm for load has been confirmed using a high-resolution transmission electron microscope (HR-TEM and HR-SEM). Dynamic light scanning (DLS) measures the average zeta potential to be -39 mV. The presence of various histological abnormalities in the livers of rats exposed to DEN/CCL_4 including regions of necrosis and apoptotic cells that are highly unusual in normal livers, could be related to the increased free radical formation during DEN/CCL_4 administration **(Habermann 1972; Park et al. 2011)**, that agree with our study there was a clear changes between studied groups when compare between the positive

control and the negative control group while in groups treated compare with the positive control group changes to be like normal. Changes in hepatic metabolism, resulting in varying levels of enzyme activity in the blood serum. Table 2 shows significant elevations in (ALT, AST, and ALP) when the positive control group was compared to the negative control group in the current study. In comparison of different treatments, we found that the sorafenib treated group showed a significant decrease in ALT and ALP levels at P values 0.035 and 0.022 respectively, compared with the positive control group. Our findings support the findings of Liu et al., 2017 **(Liu et al. 2017)**, who found that sorafenib inhibits Raf kinase and inhibits the MEK/ERK signaling pathway in liver cancer cells. The Fe2O3@Ag@Cs core shell NPs group showed a highly significant decrease at p values 0.001, 0.001, and 0.022 when compared to the positive control group, which agrees with Hoshina and Marin Morales, 2014 (**Hoshina and Marin-Morales 2014)**, who stated that silver nanoparticles have been used for cancer treatment, causing selective induction of apoptosis. According to Heinen et al., 2011 **(Heinen and da Veiga 2011**), the drug loaded on Fe2O3@Ag@Cs NPs group showed significant decrease at p values of 0.001, 0.003, and 0.001 respectively compared to the positive control group. When compared to the positive control group, the bee venom group showed a highly significant decrease in bilirubin at p value 0.001. Traditional medicine has used bee venom therapy (BVT) to treat diseases such as tumors **(Hider 1988)**. Furthermore, our findings revealed that elevated serum bilirubin levels are a common indicator of liver injury or failure. HCC invasion and replacement of liver parenchyma can result in elevated bilirubin levels **(Denora et al. 2012)**. When different treatments were compared, we discovered that the drug loading Fe2O3@Ag@Cs NPs group showed a significant decrease in bilirubin levels at a P value of 0.038 when compared to the positive control group. Sheng et al., 2017 **(Sheng et al. 2017)** found that sorafenib-incorporated nanoparticles were effective in inhibiting hepatic cancer cell proliferation. Our findings show an increase in Alpha fetoprotein (AFP) in the positive control group when compared to the negative control group. Our findings are consistent with those of Bulle F et al., 1990 **(Bulle et al. 1990)**, who reported that DEN-induced liver injury typically represents instability in the liver's metabolism, which contributes to distinct changes in the behaviors of serum enzymes. We discovered that when compared to the positive control group, all treatment groups by sorafenib, Fe2O3@Ag@Cs core shell NPs group, sorafenib loading on Fe2O3@Ag@Cs NPs group, and bee venom group showed a highly significant decrease in AFP at P value 0.001. The similarity between our findings and those of Wilhelm et al., 2008 **(Wilhelm et al., 2008)** confirmed that sorafenib inhibits tumor cell proliferation and vascularization by activating the receptor for tyrosine kinase signaling in the Ras/Raf/Mek/Erk cascade pathway. Furthermore, Zhang et al., 2011 reported that nanoparticles or nano matrix were known to improve antitumor activity in vivo. Our findings revealed that the positive control group had higher levels of malonaldehyde and nitric oxide than the negative control group, with P values of 0.001 and 0.007, respectively, in comparison to the negative control group (table 3). Our findings agreed with those of Klaunig and Kamendulis (2004) **(Klaunig and Kamendulis 2004)**, who reported that an increased level of LPO was recently reported during DEN-induced hepatocarcinogenesis. This dynamic action may also result in unrestricted free radical production, overwhelming the cellular antioxidant defensive system. When compared to the positive control group, all treatment groups sorafenib, Fe2O3@Ag@Cs core shell NPs, sorafenib loading Fe2O3@Ag@Cs NPs, and bee venom showed a significant decrease in malonaldehyde and nitric oxide levels with P values of 0.002, 0.001, 0.003, and 0.008. There was a significant drop in nitric oxide levels in the sorafenib group, drug loading Fe2O3@Ag@Cs core shell NPs group, and bee venom group compared to the positive control group, with P values of 0.007, 0.013, and 0.001 correspondingly. When compared to the positive control, our findings revealed a highly significant increase in GPx, CAT, GST, and SOD levels as important antioxidant enzymes, with P values of 0.001, 0.001, and 0.021, respectively. Our findings were consistent with those of Iacovelli et al., 2015, who discovered that sorafenib, a molecular targeted medication, improves progression-free survival and overall survival rates in cancer patients in the clinic. Poojari et al., 2016 discovered that inorganic nanoparticles significantly improved the therapeutic impact of sorafenib when compared to free sorafenib. Superparamagnetic iron oxide nanoparticles, which are commonly used as MRI contrast agents, could be co-loaded with sorafenib into solid lipid nanoparticles to improve sorafenib delivery under the guidance of remote MRI imaging, resulting in a comprehensive antitumor effect against HepG2 cells, according to.Xiao et al. **(Xiao et al., 2016)**. The nuclear and centrosome protein denticleless protein homolog is regulated by the cell cycle (DTL). DTL has been shown to play an oncogenic role in a number of cancers (Hider 1988). DUSP1 has been linked to cell cycle arrest, apoptosis, and senescence (Carmeliet and Jain 2011). According to a South Korean study, DUSP1 functioned as a tumor

suppressor during hepatocarcinogenesis, and DUSP1 expression was linked to p53 activation (Semenza 2012). According to Hao et al. 2015, disrupting a positive regulatory loop between DUSP1 and p53 accelerated HCC development and progression. When compared to the negative control group, the expression of the denticleless protein homolog (DTL) gene was found to be upregulated in the positive control group with a P value of 0.001. According to Song et al., denticleless protein homolog (DTL) is a cell cycle-regulated nuclear and centrosome protein. In osteosarcoma and colon cancer cells, siRNA suppression of DTL resulted in improved G2 arrest, p53 and p21 induction, and reduced cell proliferation, indicating that it is a significant target of miR-215. According to **Kawaguchi et al., 2015**, overexpression of DTL increased tumor cell proliferation and was associated with a malignant outcome in esophageal squamous cell carcinoma. Our findings revealed a highly significant drop in DTL level in the sorafenib group compared to the positive control group at P value 0.001, which is consistent with **Wilhelm et al., 2004**, who stated that sorafenib, a multitargeted medication, has two anticancer mechanisms. At P value 0.001, the Fe2O3@Ag@Cs core shell NPs group showed a highly significant decrease in DTL level when compared to the positive control group. Our findings were consistent with those of **Zhang et al. (2011)**, who discovered that nanoparticles or nano matrix could improve antitumor activity in vivo. At P value 0.001, the drug loading Fe2O3@Ag@Cs core shell NPs group also showed a highly significant decrease in DTL level compared to the positive control group. These findings were consistent with those of Sheng et al., 2017 **(Sheng et al. 2017),** who discovered that sorafenib nanoparticles inhibit tumor growth in vivo. Three weeks after the administration of sorafenib or sorafenib incorporated nanoparticles, hepatocellular carcinoma tissues showed signs of necrosis to varying degrees. With a P value of 0.001, the Fe2O3@Ag core shell NPs group showed a highly significant drop in DTL level when compared to the sorafenib group in our experiment. Furthermore, when compared to the sorafenib group, the loading sorafenib group showed a highly significant drop in DTL level with a P value of 0.001. According to Li et al., 2017 **(Li et al. 2017)**, superparamagnetic nanoparticles are one of the most intriguing metals due to their fictitious properties, which have been adjusted in a variety of applications. Furthermore, Kim et al., 2012 **(Kim et al. 2012)** confirmed our findings by demonstrating anticancer activity of sorafenib-incorporated DexbLG nanoparticles in human cholangiocarcinoma [HuCC-T1] cells. When compared to the positive control group, the bee venom group showed a highly significant reduction in DTL levels, with a P value of 0.001. According to Orsolic et al., 2012, bee venom and its specific components are regarded as potential cancer treatments **(Oroli 2012).** We discovered that the expression of dual specificity phosphatase 1DUSPIgene, nuclear factor of kappa light polypeptide gene enhancer in B cells inhibitor, NFKBIA gene, and suppressor of cytokine signalling 2; SOCS2 were all downregulated in the positive control group with a P value of 0.001. Our findings agreed with those of Gang et al., 2017 **(Gang et al. 2017)**, who discovered that DUSP1 plays a role in cell cycle inhibition, apoptosis, and senescence.In addition, Hao et al., 2015 **(Hao et al. 2015)** discovered that disrupting a positive regulatory loop between DUSP1 and p53 enhanced the development and progression of HCC.

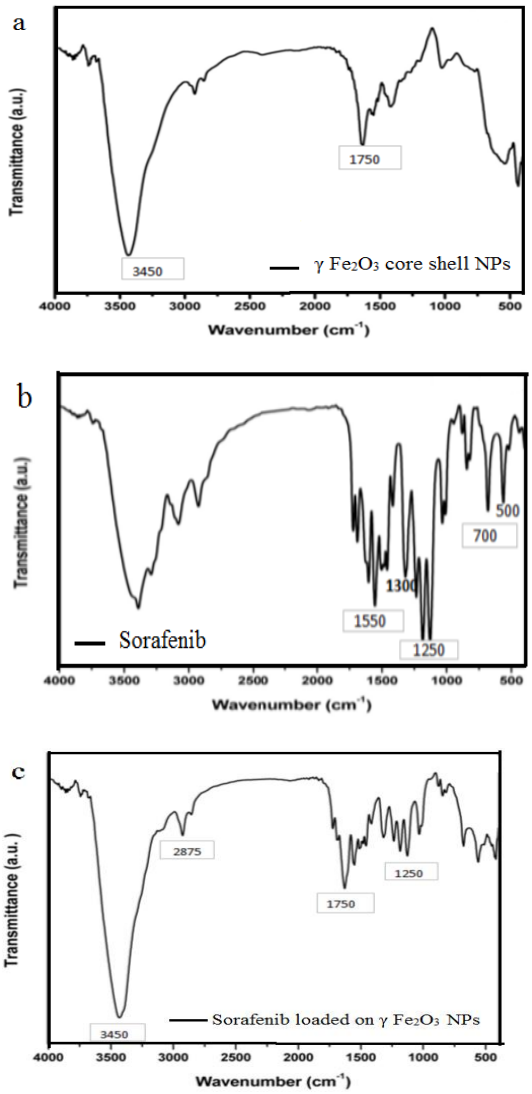

Fig.1 The transmission FTIR of (a) γ Fe_2O_3core shell nancomposite, (b) Sorafenib drug and (c) Sorafenib drug loaded on γ Fe_2O_3 NPs

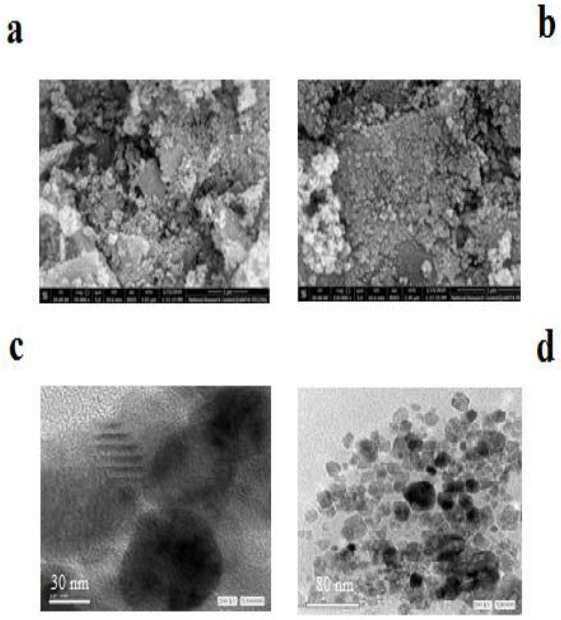

Fig. 2 High resolution transmission and scanning electron microscope of nanocomposite and the sorafenib-loaded on nanocomposite. HRSEM of a) nanocomposite, b) Sorafenib-loaded on nanocompsite, and the HRTEM of c)nanocomposite, d) drug-loaded-nanocomposite

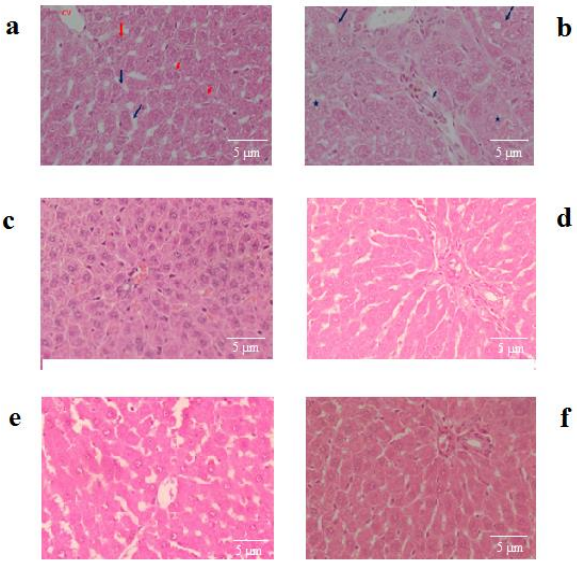

Fig. 3 (a) A section from liver of negative control group showing normal hepatic lobule .The hepatocytes (arrows) radiated from the central vein (CV). The hepatocytes showing vesicular nuclei (arrows), some of it are binucleated (arrowheads) and are separated with sinusoids (blue arrow), (b) liver of positive control group showing tumor cells appeared like pseudo-glands (arrows). Fibrosis sheet (arrowhead) and focal necrosis (asterisk) are seen, (c) liver of treated group by 10 mg/Kg b.wt. sorafenib, (d) liver of group treated by SPION@Ag core shell nanoparticles, (e) liver of group treated by core shell nanoparticles loaded with sorafenib drug, (f) liver of group treated by bee venom (H&E stain, Scale bar: 5 µm).

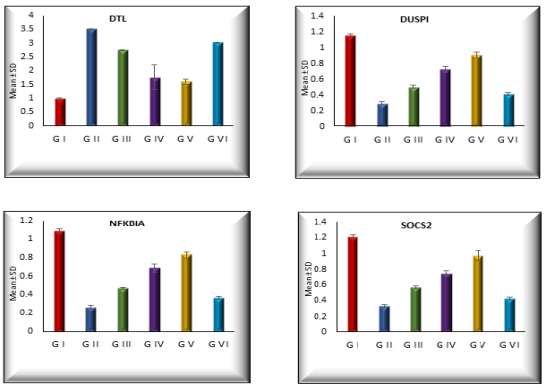

Fig.4 Show qRT-PCR gene expression of DTL, DUSP1, NFKBIA, SOCS2

Kato et al. (2013) discovered that DUSP1 functions as a tumor suppressor during hepatocarcinogenesis and that its expression is associated with p53 activation. According to Wei et al., 2015, MiR 101 inhibited macrophage-induced HCC tumor formation by regulating tumor growth factor release via DUSP1 targeting. According to **Wang et al., 2015,** liver cancer tissue has lower NFKBIA expression than control tissue, and negative NFKBIA expression predicts poor prognosis in people with primary HCC.SOCS2 has been found to suppress tumor metastasis, according to and Cui et al., 2016 **(Cui et al., 2016)**. According to Qiu et al., 2013, SOCS2 expression has been shown to be dramatically reduced in HCC, which has been linked to aggressive tumor development and poor prognosis in HCC patients (Qiu et al. 2013) Our findings revealed a significant increase in DUSPI, NFKBIA, and SOCS2 gene levels in the sorafenib-treated group, Fe2O3@Ag@Cs core shell NPs-treated group, and loading Fe2O3@Ag@Cs NPs-treated group when compared to the positive control group at P value 0.001. Furthermore, when the loaded Fe2O3@Ag@Cs core shell NPs group was compared to the sorafenib group, the loaded Fe2O3@Ag@Cs core shell NPs group showed a very significant increase in DUSPI,NFKBIA, and SOCS2 gene levels, with a P value of 0.001.

Our findings were similar to those of Wilhelm et al. (2004), who discovered that sorafenib, a new multitargeted medication, has two anticancer mechanisms. Furthermore, Hu et al., 2012 **(Hu et al.**

2012) discovered that in patients with HCC who received a liver transplant, those given oral sorafenib had significantly higher disease free survival (DFS) and overall survival (OS) than the control group. Furthermore, our findings, which were confirmed by **Zhang et al., 2011**, demonstrated that nanoparticles or nano matrix may enhance anticancer activity in vivo. At P value 0.001, we found a highly significant increase in DUSPI, NFKBIA, and SOCS2 gene levels in the Fe2O3@Ag@Cs core shell treated NPs group when compared to the Fe2O3@Ag@Cs core shell treated group and the sorafenib group. Kim et al., 2012 **(Kim et al. 2012)** agreed with our findings, concluding that sorafenib-incorporated DexbLG nanoparticles outperformed sorafenib alone in vitro. Sheng et al., 2017 discovered that nanoparticles containing sorafenib were effective in inhibiting the proliferation of liver cancer cells. Our data revealed a significant increase in DUSPI, NFKBIA, and SOCS2 gene levels in the Bee venom treatment group when compared to the positive control group, with a P value of 0.001. According to Heinen et al., 2011 **(Heinen and da Veiga 2011)**, bee venom has cancer-fighting properties such as induction of apoptosis, necrosis, cytotoxicity, and suppression of proliferation in a variety of cancer cell types such as prostate, breast, lung, liver, and bladder. Furthermore, Orsolic et al., 2012 **(Oroli, 2012)** discovered that bee venom and its specific components are promising cancer treatment agents.

Table 1 Primer sequences used for qPCR, F: forward primer; R: reverse primer; (DTL) denticleless protein homolog; (DUSP1) dual specificity phosphatase 1; (NFKBIA) nuclear factor of k light chain gene enhancer in B cells inhibitor, α; (SOCS2) suppressor of cytokine signaling 2.

Gene	Primer sequence (5′–3′)	References
DTL	F- CCT CTG TCC GAT CCT CCA AA R- AAA GAT TTT CAG TCC CGC GG	**(Meng et al. 2018)**
DUSP1	F- AGA ATG TTC CTG ACT CGG CA R- AAG CAA AAT CCA ATC CCG GG	**(Meng et al. 2018)**
NFKBIA	F- AGC GAT GGG GTC TCA CTA TG R- TCC AAC AGC TTA GGT CAG GG	**(Meng et al. 2018)**
SOCS2	F- GCT TGG GGT TAA ATG GTG CA R- AAG GGA TGG GGC TCT TTC TC	**(Meng et al. 2018)**
β-actin	F-GGT ATG GAA TCC TGT GGC ATC CAT GAA A R-GTG TAA AAC GCA GCT CAG TAA CAG TCC G	**(Serrano et al. 2005)**

Table 2 Each value represents mean±SD. (a) significant compared with group I (Negative control), (b) significant compared with group II (Positive control), (c) significant compared with group III (HCC + sorafenib), (d) significant compared with group IV (HCC + γ Fe_2O_3@Ag NPs), (e) significant compared with group V (HCC + γ Fe_2O_3@Ag NPs loaded with sorafenib) and (f) significant compared with group VI (HCC+ bee venom)

		G (I)	G (II)	G (III)	G (IV)	G (V)	G (VI)
Liver index	Mean±SD	2.541± 0.415	4.246± 0.326 [a]	2.876± 0.259 [b]	2.787± 0.229 [b]	2.917± 0.316 [b]	3.596± 0.40 [a,b,c,d,e,f]
ALT (U/l)	Mean±SD	50.143± 5.551	92.857± 12.103 [a]	72.0± 10.312 [a,b]	41.286± 9.160 [b,c]	47.0± 17.588 [b,c]	57.286± 15.435 [b]
AST (U/l)	Mean±SD	257.571± 42.019	415.143± 66.529 [a]	302.571± 69.935	230.286± 66.35 [b]	252.286± 95.280 [b]	312.143± 95.801
Bil (mg/dL)	Mean± SD	0.026± 0.005	0.033± 0.010	0.024± 0.005	0.023± 0.008	0.021± 0.007 [b]	0.014± 0.005 [a,b]
ALP (U/l)	Mean±SD	202.143± 61.061	380.000± 79.044[a,c]	280.0± 72.402 [b,d,e,f]	105.857± 38.085 [a,b,c]	142.571± 34.078 [b,c]	185.714± 30.071 [b,c]
AFP (ng/ml)	Mean±SD	0.171± 0.076	10.429± 1.272 [a]	0.486± 0.241 [b,d,e,f]	0.30± 0.141	0.443± 0.113	0.429± 0.111

Table 3 Each value represents mean±SD. (a) significant compared with group I (Negative control), (b) significant compared with group II (Positive control), (c) significant compared with group III (HCC + sorafenib), (d) significant compared with group IV (HCC + γ Fe2O3@Ag NPs), (e) significant compared with group V (HCC + γ Fe2O3@Ag NPs loaded with sorafenib) and (f) significant compared with group VI (HCC+ bee venom)

		G (I)	G (II)	G (III)	G (IV)	G (V)	G (VI)
MDA nmol/g.tissue	Mean±SD	10.286± 3.684	22.571± 8.715 [a]	12.571± 1.512 [b]	10.286± 3.450	12.857± 3.436 [b]	13.714± 2.059 [b]
NO µmol/L	Mean±SD	8.114± 1.685	11.400± 1.033 [a]	9.229± 0.976 [b]	10.214± 0.135 [a]	9.357± 1.045 [b]	8.329± 1.023 [b,d]
GPx U/gT	Mean±SD	8.286± 1.799	7.143± 2.268	10.714± 1.113 [b]	16.0± 3.830 [a,b,c]	11.143± 0.90 [b,d]	11.857± 0.90 [a,b,d]
CAT U/g	Mean±SD	0.059± 0.013	0.031± 0.009	0.080± 0.013 [b]	0.120± 0.049 [a,b,c]	0.091± 0.020 [b]	0.074± 0.014 [b,d]

G-S-transferase (U/g tissue)	Mean±SD	12.271± 0.892	7.571± 1.512 [a]	9.271± 2.341 [a]	10.271± 0.111 [b]	10.514± 0.267 [b]	10.114± 1.795 [b]
SOD U/gm tissue	Mean±SD	383.571± 77.833	321.571± 32.700	347.0± 56.220	395.0± 54.108	424.143± 29.060 [b]	388.0+ 65.343

Table 4 Each value represents mean±SD. (a) significant compared with group I (Negative control), (b) significant compared with group II (Positive control), (c) significant compared with group III (HCC + sorafenib), (d) significant compared with group IV (HCC + γ Fe_2O_3@Ag NPs), (e) significant compared with group V (HCC + γ Fe_2O_3@Ag loaded with sorafenib) and (f) significant compared with group VI (HCC+ bee venom)

		G (I)	G (II)	G (III)	G (IV)	G (V)	G (VI)
DTL	Mean±SD	1± 0.02	3.511± 0.022 [a]	2.750± 0.022 [a,b]	1.760± 0.448 [a,b,c]	1.616± 0.097 [a,b,c]	3.023± 0.02 [a,b,d,e]
DUSPI	Mean±SD	1.156± 0.017	0.29± 0.02 [a]	0.500± 0.022 [a,b]	0.721± 0.036 [a,b,c]	0.903± 0.036 [a,b,c,d]	0.407± 0.018 [a,b,c,d,e]
NFKBIA	Mean±SD	1.090± 0.022	0.260± 0.022 [a]	0.466± 0.011 [a,b]	0.689± 0.042 [a,b,c]	0.833± 0.037 [a,b,c,d]	0.364± 0.017 [a,b,c,d,e]
SOCS2	Mean±SD	1.210± 0.022	0.33± 0.022 [a]	0.566± 0.017 [a,b]	0. 0.743± 0.038 [a,b,c]	0.973± 0.058 [a,b,c,d]	0.424± 0.017 [a,b,c,d,e]

Conclusion

Sorafenib drug delivery has been accomplished by loading it on synthetic ecofriendly core shell nanoparticles. The uniqueness of our solution stems from the fact that the loading drug is a promising anticancer agent with an appealing role in sorafenib targeting. It outperforms bee venom as a standard cancer treatment while also lowering the therapeutic dosage and, as a result, the adverse effects. Furthermore, it achieved a significant variation in the fold of expression in our studied genes DTL, DUSP1, NFKBIA, and SOCS2, which is closely related to the degree of pathogenicity of hepatocellular carcinoma and provides a valuable insight into the progression of HCC and prognosis, proving our suggestion of the role of sorafenib when compared with bee venom.

Acknowledgement

The authors would like to thank the National Research Centre for the financial support through the work of synthesis, characterization of nanocomposite and do the experimental animal.

Conflict of interest: The authors declare that there are no conflicts of interest.

4. References

Aebi H (1984) Catalase in vitro. Methods Enzymol 105:121–126. https://doi.org/10.1016/s0076-6879(84)05016-3

Alexiou C, Arnold W, Klein RJ, et al (2000) Locoregional cancer treatment with magnetic drug targeting. Cancer Res 60:6641–6648

Arruebo M, Fernández-Pacheco R, Ibarra MR, Santamaría J (2007) Magnetic nanoparticles for drug delivery. Nano Today 2:22–32. https://doi.org/10.1016/S1748-0132(07)70084-1

Bishayee A, Dhir N (2009) Resveratrol-mediated chemoprevention of diethylnitrosamine-initiated hepatocarcinogenesis: inhibition of cell proliferation and induction of apoptosis. Chem Biol Interact 179:131–144. https://doi.org/10.1016/j.cbi.2008.11.015

Bulle F, Mavier P, Zafrani ES, et al (1990) Mechanism of gamma-glutamyl transpeptidase release in serum during intrahepatic and extrahepatic cholestasis in the rat: a histochemical, biochemical and molecular approach. Hepatology 11:545–550. https://doi.org/10.1002/hep.1840110404

Carmeliet P, Jain RK (2011) Molecular mechanisms and clinical applications of angiogenesis. Nature 473:298–307. https://doi.org/10.1038/nature10144

Chauhan VP, Jain RK (2013) Strategies for advancing cancer nanomedicine. Nat Mater 12:958–962. https://doi.org/10.1038/nmat3792

Cheng W, Nie J, Gao N, et al (2017) A Multifunctional Nanoplatform against Multidrug Resistant Cancer: Merging the Best of Targeted Chemo/Gene/Photothermal Therapy. Advanced Functional Materials 27:1704135. https://doi.org/10.1002/adfm.201704135

Cui M, Sun J, Hou J, et al (2016) The suppressor of cytokine signaling 2 (SOCS2) inhibits tumor metastasis in hepatocellular carcinoma. Tumour Biol 37:13521–13531. https://doi.org/10.1007/s13277-016-5215-7

Denora N, Cassano T, Laquintana V, et al (2012) Novel codrugs with GABAergic activity for dopamine delivery in the brain. Int J Pharm 437:221–231. https://doi.org/10.1016/j.ijpharm.2012.08.023

Ding X-X, Zhu Q-G, Zhang S-M, et al (2017) Precision medicine for hepatocellular carcinoma: driver mutations and targeted therapy. Oncotarget 8:55715–55730. https://doi.org/10.18632/oncotarget.18382

du M, Xu Y, Zhang H, et al (2010) Selective Synthesis of Fe2O3 and Fe3O4 Nanowires Via a Single Precursor: A General Method for Metal Oxide Nanowires. Nanoscale research letters 5:1295–300. https://doi.org/10.1007/s11671-010-9641-y

Evanoff DD, Chumanov G (2005) Synthesis and optical properties of silver nanoparticles and arrays. Chemphyschem 6:1221–1231. https://doi.org/10.1002/cphc.200500113

Fanizza E, Iacobazzi RM, Laquintana V, et al (2016) Highly selective luminescent nanostructures for mitochondrial imaging and targeting. Nanoscale 8:3350–3361. https://doi.org/10.1039/C5NR08139D

Fattovich G, Stroffolini T, Zagni I, Donato F (2004) Hepatocellular carcinoma in cirrhosis: incidence and risk factors. Gastroenterology 127:S35-50. https://doi.org/10.1053/j.gastro.2004.09.014

Ferrari M (2005) Cancer nanotechnology: opportunities and challenges. Nat Rev Cancer 5:161–171. https://doi.org/10.1038/nrc1566

Gang L, Qun L, Liu W-D, et al (2017) MicroRNA-34a promotes cell cycle arrest and apoptosis and suppresses cell adhesion by targeting DUSP1 in osteosarcoma. Am J Transl Res 9:5388–5399

Goswami N, Luo Z, Yuan X, et al (2017) Engineering gold-based radiosensitizers for cancer radiotherapy. Mater Horiz 4:817–831. https://doi.org/10.1039/C7MH00451F

Habermann E (1972) Bee and wasp venoms. Science 177:314–322. https://doi.org/10.1126/science.177.4046.314

Habig WH, Pabst MJ, Jakoby WB (1974) Glutathione S-transferases. The first enzymatic step in mercapturic acid formation. J Biol Chem 249:7130–7139

Hao P-P, Li H, Lee M-J, et al (2015) Disruption of a regulatory loop between DUSP1 and p53 contributes to hepatocellular carcinoma development and progression. J Hepatol 62:1278–1286. https://doi.org/10.1016/j.jhep.2014.12.033

Heinen TE, da Veiga ABG (2011) Arthropod venoms and cancer. Toxicon 57:497–511. https://doi.org/10.1016/j.toxicon.2011.01.002

Henry RJ, Chiamori N, Golub OJ, Berkman S (1960) Revised spectrophotometric methods for the determination of glutamic-oxalacetic transaminase, glutamic-pyruvic transaminase, and lactic acid dehydrogenase. Am J Clin Pathol 34:381–398. https://doi.org/10.1093/ajcp/34.4_ts.381

Hider RC (1988) Honeybee venom: A rich source of pharmacologically active peptides. Endeavour 12:60–65. https://doi.org/10.1016/0160-9327(88)90082-8

Hoshina MM, Marin-Morales MA (2014) Anti-genotoxicity and anti-mutagenicity of Apis mellifera venom. Mutat Res Genet Toxicol Environ Mutagen 762:43–48. https://doi.org/10.1016/j.mrgentox.2013.11.005

Hu A-B, He X-S, Tai Q, et al (2012) [Efficacy and safety of sorafenib in the prevention and treatment of hepatocellular carcinoma recurrences after liver transplantation]. Zhonghua yi xue za zhi 92:1264–7. https://doi.org/10.3760/cma.j.issn.0376-2491.2012.18.012

Iacovelli R, Sternberg CN, Porta C, et al (2015) Inhibition of the VEGF/VEGFR pathway improves survival in advanced kidney cancer: a systematic review and meta-analysis. Curr Drug Targets 16:164–170. https://doi.org/10.2174/1389450115666141120120145

Jain RK (2013) Normalizing Tumor Microenvironment to Treat Cancer: Bench to Bedside to Biomarkers. JCO 31:2205–2218. https://doi.org/10.1200/JCO.2012.46.3653

Kato I, Maita H, Takahashi-Niki K, et al (2013) Oxidized DJ-1 inhibits p53 by sequestering p53 from promoters in a DNA-binding affinity-dependent manner. Mol Cell Biol 33:340–359. https://doi.org/10.1128/MCB.01350-12

Kim DH, Kim M-D, Choi C-W, et al (2012) Antitumor activity of sorafenib-incorporated nanoparticles of dextran/poly(dl-lactide-co-glycolide) block copolymer. Nanoscale Research Letters 7:91. https://doi.org/10.1186/1556-276X-7-91

Kj L, An D, Tm P (2015) Epidemiology of hepatocellular carcinoma. Surgical oncology clinics of North America 24:. https://doi.org/10.1016/j.soc.2014.09.001

Klaunig JE, Kamendulis LM (2004) The role of oxidative stress in carcinogenesis. Annu Rev Pharmacol Toxicol 44:239–267. https://doi.org/10.1146/annurev.pharmtox.44.101802.121851

Kumar A, Jena PK, Behera S, et al (2010) Multifunctional magnetic nanoparticles for targeted delivery. Nanomedicine 6:64–69. https://doi.org/10.1016/j.nano.2009.04.002

Kydd J, Jadia R, Velpuri P, et al (2017) Targeting Strategies for the Combination Treatment of Cancer Using Drug Delivery Systems. Pharmaceutics 9:46. https://doi.org/10.3390/pharmaceutics9040046

Laquintana V, Denora N, Lopalco A, et al (2014) Translocator protein ligand-PLGA conjugated nanoparticles for 5-fluorouracil delivery to glioma cancer cells. Mol Pharm 11:859–871. https://doi.org/10.1021/mp400536z

Li D, Su J, Yang J, et al (2017) Optical surface plasmon resonance sensor modified by mutant glucose/galactose-binding protein for affinity detection of glucose molecules. Biomed Opt Express, BOE 8:5206–5217. https://doi.org/10.1364/BOE.8.005206

Liu G, Tsai H, Zeng X, et al (2017) Phosphorylcholine-based stealthy nanocapsules enabling tumor microenvironment-responsive doxorubicin release for tumor suppression. Theranostics 7:1192–1203. https://doi.org/10.7150/thno.17881

Liu G, Tsai HI, Zeng X, et al (2019) Black phosphorus nanosheets-based stable drug delivery system via drug-self-stabilization for combined photothermal and chemo cancer therapy. Chemical Engineering Journal. https://doi.org/10.1016/j.cej.2019.121917

Luo M, Cheng W, Zeng X, et al (2019) Folic Acid-Functionalized Black Phosphorus Quantum Dots for Targeted Chemo-Photothermal Combination Cancer Therapy. Pharmaceutics 11:242. https://doi.org/10.3390/pharmaceutics11050242

Marková Z, Siskova K, Filip J, et al (2012) Chitosan-based synthesis of magnetically-driven nanocomposites with biogenic magnetite core, controlled silver size, and high antimicrobial activity. Green Chem 14:2550–2558. https://doi.org/10.1039/C2GC35545K

Mascolo MC, Pei Y, Ring TA (2013) Room Temperature Co-Precipitation Synthesis of Magnetite Nanoparticles in a Large pH Window with Different Bases. Materials (Basel) 6:5549–5567. https://doi.org/10.3390/ma6125549

Moradpour D, Blum HE (2005) Pathogenesis of hepatocellular carcinoma. Eur J Gastroenterol Hepatol 17:477–483. https://doi.org/10.1097/00042737-200505000-00002

Nishikimi M, Appaji N, Yagi K (1972) The occurrence of superoxide anion in the reaction of reduced phenazine methosulfate and molecular oxygen. Biochem Biophys Res Commun 46:849–854. https://doi.org/10.1016/s0006-291x(72)80218-3

Ohkawa H, Ohishi N, Yagi K (1979) Assay for lipid peroxides in animal tissues by thiobarbituric acid reaction. Anal Biochem 95:351–358. https://doi.org/10.1016/0003-2697(79)90738-3

Oršolić N (2012) Bee venom in cancer therapy. Cancer Metastasis Rev 31:173–194. https://doi.org/10.1007/s10555-011-9339-3

Owen J, Rademeyer P, Chung D, et al (2015) Magnetic targeting of microbubbles against physiologically relevant flow conditions. Interface Focus 5:20150001. https://doi.org/10.1098/rsfs.2015.0001

Pablico-Lansigan MH, Situ SF, Samia ACS (2013) Magnetic particle imaging: advancements and perspectives for real-time in vivo monitoring and image-guided therapy. Nanoscale 5:4040–4055. https://doi.org/10.1039/C3NR00544E

Paglia DE, Valentine WN (1967) Studies on the quantitative and qualitative characterization of erythrocyte glutathione peroxidase. J Lab Clin Med 70:158–169

Park J-H, Kum Y-S, Lee T-I, et al (2011) Melittin attenuates liver injury in thioacetamide-treated mice through modulating inflammation and fibrogenesis. Exp Biol Med (Maywood) 236:1306–1313. https://doi.org/10.1258/ebm.2011.011127

Poojari R, Kini S, Srivastava R, Panda D (2016) Intracellular interactions of electrostatically mediated layer-by-layer assembled polyelectrolytes based sorafenib nanoparticles in oral cancer cells. Colloids Surf B Biointerfaces 143:131–138. https://doi.org/10.1016/j.colsurfb.2016.03.024

Prijic S, Sersa G (2011) Magnetic nanoparticles as targeted delivery systems in oncology. Radiol Oncol 45:1–16. https://doi.org/10.2478/v10019-011-0001-z

Qiu X, Zheng J, Guo X, et al (2013) Reduced expression of SOCS2 and SOCS6 in hepatocellular carcinoma correlates with aggressive tumor progression and poor prognosis. Mol Cell Biochem 378:99–106. https://doi.org/10.1007/s11010-013-1599-5

Ravichandran M, Oza G, Tapia J, et al (2016) Plasmonic/Magnetic Multifunctional nanoplatform for Cancer Theranostics. Scientific Reports 6:34874. https://doi.org/10.1038/srep34874

Redolfi Riva E, Pastoriza-Santos I, Lak A, et al (2017) Plasmonic/magnetic nanocomposites: Gold nanorods-functionalized silica coated magnetic nanoparticles. Journal of Colloid and Interface Science 502:201–209. https://doi.org/10.1016/j.jcis.2017.04.089

Sayed D (2019) The protective effect of Nigella sativa oil against reproductive toxicity, hormonal alterations, and oxidative damage induced by Sertraline in male rats. THE EGYPTIAN JOURNAL OF EXPERIMENTAL BIOLOGY (Zoology) 15:. https://doi.org/10.5455/egysebz.20190325113108

Semenza GL (2012) Hypoxia-inducible factors in physiology and medicine. Cell 148:399–408. https://doi.org/10.1016/j.cell.2012.01.021

Setyawati MI, Yuan X, Xie J, Leong DT (2014) The influence of lysosomal stability of silver nanomaterials on their toxicity to human cells. Biomaterials 35:6707–6715. https://doi.org/10.1016/j.biomaterials.2014.05.007

Sharaf SMA, Abbas HS, Ismaeil TAM (2019) Characterization of spirugenic iron oxide nanoparticles and their antibacterial activity against multidrug-resistant Helicobacter pylori. Egyptian Journal of Phycology 20:1–28. https://doi.org/10.21608/egyjs.2019.116018

Shawi OEE, El-Rahman SSA, Hameed MAE (2015) Reishi Mushroom Attenuates Hepatic Inflammation and Fibrosis Induced by Irradiation Enhanced Carbon Tetrachloride in Rat Model. Journal of Biosciences and Medicines 3:24–38. https://doi.org/10.4236/jbm.2015.310004

Sheng X, Huang T, Qin J, et al (2017) Preparation, pharmacokinetics, tissue distribution and antitumor effect of sorafenib-incorporating nanoparticles in vivo. Oncol Lett 14:6163–6169. https://doi.org/10.3892/ol.2017.6934

Shi J, Kantoff PW, Wooster R, Farokhzad OC (2017) Cancer nanomedicine: progress, challenges and opportunities. Nat Rev Cancer 17:20–37. https://doi.org/10.1038/nrc.2016.108

Song B, Wang Y, Titmus MA, et al (2010) Molecular mechanism of chemoresistance by miR-215 in osteosarcoma and colon cancer cells. Molecular Cancer 9:96. https://doi.org/10.1186/1476-4598-9-96

Song X-R, Goswami N, Yang H-H, Xie J (2016) Functionalization of metal nanoclusters for biomedical applications. Analyst 141:3126–3140. https://doi.org/10.1039/C6AN00773B

Srinivasan SY, Paknikar KM, Bodas D, Gajbhiye V (2018) Applications of cobalt ferrite nanoparticles in biomedical nanotechnology. Nanomedicine (Lond) 13:1221–1238. https://doi.org/10.2217/nnm-2017-0379

Stafford S, Serrano Garcia R, Gun'ko YK (2018) Multimodal Magnetic-Plasmonic Nanoparticles for Biomedical Applications. Applied Sciences 8:97. https://doi.org/10.3390/app8010097

Valente G, Depalo N, Paola I de, et al (2016) Integrin-targeting with peptide-bioconjugated semiconductor-magnetic nanocrystalline heterostructures. Nano Research 9:644–662. https://doi.org/10.1007/s12274-015-0944-2

Wang X, Xiong L, Yu G, et al (2015) Cathepsin S silencing induces apoptosis of human hepatocellular carcinoma cells. Am J Transl Res 7:100–110

Wei X, Tang C, Lu X, et al (2015) MiR-101 targets DUSP1 to regulate the TGF-β secretion in sorafenib inhibits macrophage-induced growth of hepatocarcinoma. Oncotarget 6:18389–18405

Wilhelm SM, Adnane L, Newell P, et al (2008) Preclinical overview of sorafenib, a multikinase inhibitor that targets both Raf and VEGF and PDGF receptor tyrosine kinase signaling. Mol Cancer Ther 7:3129–3140. https://doi.org/10.1158/1535-7163.MCT-08-0013

Wilhelm SM, Carter C, Tang L, et al (2004) BAY 43-9006 exhibits broad spectrum oral antitumor activity and targets the RAF/MEK/ERK pathway and receptor tyrosine kinases involved in tumor progression and angiogenesis. Cancer Res 64:7099–7109. https://doi.org/10.1158/0008-5472.CAN-04-1443

Xiao Y, Liu Y, Yang S, et al (2016) Sorafenib and Gadolinium co-loaded liposomes for drug delivery and MRI-guided HCC treatment. Colloids and Surfaces B: Biointerfaces 141:. https://doi.org/10.1016/j.colsurfb.2016.01.016

Young DS (1997) Effects of drugs on clinical laboratory tests. Ann Clin Biochem 34 (Pt 6):579–581. https://doi.org/10.1177/000456329703400601

Zhang J-Y, He B, Qu W, et al (2011) Preparation of the albumin nanoparticle system loaded with both paclitaxel and sorafenib and its evaluation in vitro and in vivo. J Microencapsul 28:528–536. https://doi.org/10.3109/02652048.2011.590614

Zhang X, Niu Y, Meng X, et al (2013) Structural evolution and characteristics of the phase transformations between α-Fe2O3, Fe3O4 and γ-Fe2O3 nanoparticles under reducing and oxidizing atmospheres. CrystEngComm 15:8166. https://doi.org/10.1039/c3ce41269e

Zhang X-D, Luo Z, Chen J, et al (2014) Ultrasmall Au(10-12)(SG)(10-12) nanomolecules for high tumor specificity and cancer radiotherapy. Adv Mater 26:4565–4568. https://doi.org/10.1002/adma.201400866

Zheng K, Setyawati MI, Leong DT, Xie J (2017) Antimicrobial Gold Nanoclusters. ACS Nano 11:6904–6910. https://doi.org/10.1021/acsnano.7b02035

Zheng K, Setyawati MI, Lim T-P, et al (2016) Antimicrobial Cluster Bombs: Silver Nanoclusters Packed with Daptomycin. ACS Nano 10:7934–7942. https://doi.org/10.1021/acsnano.6b03862

Zielonka A, Klimek-Ochab M (2017) Fungal synthesis of size-defined nanoparticles. Adv Nat Sci: Nanosci Nanotechnol 8:043001. https://doi.org/10.1088/2043-6254/aa84d4